Comput Geosci (2011) 15:421–429
DOI 10.1007/s10596-010-9212-4

ORIGINAL PAPER

Application of EM algorithms for seismic facices classification

Mei Han · Yong Zhao · Gaoming Li · Albert C. Reynolds

Received: 25 August 2009 / Accepted: 4 October 2010 / Published online: 23 October 2010

Abstract Identification of the geological facies and their distribution from seismic and other available geological information is important during the early stage of reservoir development (e.g. decision on initial well locations). Traditionally, this is done by manually inspecting the signatures of the seismic attribute maps, which is very time-consuming. This paper proposes an application of the Expectation-Maximization (EM) algorithm to automatically identify geological facies from seismic data. While the properties within a certain geological facies are relatively homogeneous, the properties between geological facies can be rather different. Assuming that noisy seismic data of a geological facies, which reflect rock properties, can be approximated with a Gaussian distribution, the seismic data of a reservoir composed of several geological facies are samples from a Gaussian mixture model. The mean of each Gaussian model represents the average value of the seismic data within each facies while the variance gives the variation of the seismic data within a facies. The proportions in the Gaussian mixture model represent the relative volumes of different facies in the reservoir. In this setting, the facies classification problem becomes a problem of estimating the parameters defining the Gaussian mixture model. The EM algorithm has long been used to estimate Gaussian mixture model parameters. As the standard EM algorithm does not consider spatial relationship among data, it can generate spatially scattered seismic facies which is physically unrealistic. We improve the standard EM algorithm by adding a spatial constraint to enhance spatial continuity of the estimated geological facies. By applying the EM algorithms to acoustic impedance and Poisson's ratio data for two synthetic examples, we are able to identify the facies distribution.

Keywords EM · Facies · Poison's ratio · Acoustic impedance

1 Introduction

Traditionally, stratigraphic reservoir characterization is conducted within the framework of depositional environment and facies models. In order to obtain a reasonable reservoir description, it is desirable to integrate all available data to identify and map rock facies. Usually, facies identification is done by manually analyzing core, well log and seismic data, which requires time and experience and does not necessarily guarantee consistent results from different sources of data. Liu and Oliver [15] and Zhao et al. [24] applied the ensemble Kalman filter method to assimilate the production and seismic data for mapping the rock facies. However, these methods require core, logging and production data and they can only be applied after the wells are drilled and the reservoir is put on production in the development phase. As drilling wildcat wells is risky and expensive, it is important to identify the distribution of rock facies based on seismic data obtained during exploration, which is the focus of this paper.

M. Han · G. Li (✉) · A. C. Reynolds
University of Tulsa, 800 S. Tucker Dr.,
Tulsa, OK 74104 USA
e-mail: gaoming-li@utulsa.edu

Y. Zhao
600 North Dairy Ashford (77079-1175) P.O. Box 2197,
Houston, TX 77252 USA

Recently, geostatistics and artificial neural networks (ANN) [4, 20] have been applied to integrate seismic data with properties measured at well locations to identify geological facies. Arpat et al. [4] proposed a neural network based automation method that learns how to relate the seismic data to facies. The neural net is trained by the interpreted facies results of a small portion of seismic data by expert geologists. The trained ANN is then applied to the remaining portion of the data to automatically detect geological facies. The ANN technique together with a beta-Bayesian method (BBM) and a discriminant analysis (DA) algorithm is also applied in [20] to link the geological facies observations at well locations using seismic data. Geostatistical inversion was used to estimate the conditional probabilities of facies occurrence given residual thickness. The examples in both papers show some success. However, the reliable application of neural networks requires a significant training effort and a large amount of training time, especially for large data sets.

Another way to identify geological facies from seismic data is to apply data clustering and closely related image segmentation algorithms. These techniques have been widely used in data mining and image processing [3, 17, 18, 22]. John et al. [13] applied a simple form of Bayes theorem to compute the probability of occurrence of each facies at measured locations of acoustic impedance. In this method, an optimization algorithm is applied to estimate the parameters of the Gaussian mixture model (mean, standard deviation and prior probability of each facies) that best fits the data histogram. As the number of facies (Gaussian models) is unknown, it is necessary to repeat the optimization procedure with different specified number of facies and choose the one that best fits the data histogram. The method ignores the spatial continuity of each facies and it can only incorporate one type of data. Teixeira et al. [21] presented a method based on Bayesian theory to infer subsurface lithofacies and initial fluid distribution by integrating different data sources, such as well log data and seismic attributes. An Expectation-Maximization (EM) algorithm was applied to classify facies from three types of logs at different wells. The facies classification result is then used as prior information to further estimate facies distribution from seismic data. As in [13], the uncertainty on the number of Gaussian models (facies) and the spatial continuity are not considered.

Zhao et al. [25] applied a spatial EM algorithm to group seismic and production data for the purpose of estimating measurement error. The EM algorithm in [25] is somewhat similar to that used in [13]. However, EM algorithm can incorporate different types of data and the improved version of the algorithm (spatial EM) incorporates the spatial information among data to enhance the spatial continuity among groups. Here, a group is refereed to as the data that sampled from one Gaussian model or a geological facies. Another advantage of the Zhao et al. methodology is that it does not require a priori knowledge of the number of facies and does not require repeating the same procedure with a different number of groups as in [13]. Instead, it starts with a large number of groups and automatically deletes spatially discontinuous groups during the optimization process.

The EM algorithm gained its notoriety in statistics for parameter estimation. To the best of our knowledge, Hartley [12] was the first one to introduce the concept of EM. However, Dempster et al. [8] formalized and applied this method. Since then, EM has been applied to signal processing, pattern recognition, image restoration and reconstruction [14, 16, 19]. In essence, the EM algorithm is an iterative optimization method for parameter estimation. There are two steps at each iteration: 1) With the estimate of the Gaussian mixture model parameters from the previous iteration, the membership information (i.e. the probability that each datum is sampled from each Gaussian model) is estimated. This step is referred to as the expectation step, or simply the E-step. 2) Using the estimated membership information and the measurements, a maximum likelihood estimate of the Gaussian mixture model parameters is obtained in the second step. This step is referred to as the maximization step or simply the M-step. This two-step process is updated at each iteration until convergence is achieved.

When the standard EM algorithm is applied to data with spatial continuity, it gathers all the data with similar amplitude together regardless of their spatial locations. This can result in facies that contain data sparsely distributed in space. To overcome this disadvantage, some strategies have been put forward to construct the spatially-constrained EM algorithm in the literature. Diplaros et al. [9] proposed to smooth the membership matrix, in which the entries represent the probability that each datum samples from each Gaussian model (group). The basic idea of smoothing the membership matrix is to ensure data points that are spatially close to each other have similar probability of falling into the same group. In the spatially-constrained EM algorithm used by [9], a smoothing step is added between the E-step and M-step. Besag et al. [5] forced spatial continuity within each group by conditionally approximating the local Markov random field. Allard and Guillot [1] applied a version of the Classification EM algorithm

(CEM) [7] to group data in regions of irregularly shapes and recover the spatial correlation of measurements within each group. These algorithms assume that the measurements in each group are spatially correlated. The neighborhood EM (NEM) algorithm [2] ensures the spatial continuity of each group by adding a spatial penalty term to the log-likelihood function to be optimized. When two data points are far away in space, the penalty term prevents them from falling into the same group. In this paper, we apply three different EM algorithms: the standard EM algorithm without any spatial constraint, the neighborhood EM (NEM) algorithm and the spatial EM algorithm developed in [23] and [25] to estimate the distribution of maps of facies from seismic data.

2 Gaussian mixture model

In statistics, a Gaussian mixture model is a probability distribution that is a convex combination of some Gaussian probability distributions. Suppose that a random measurement d represents a sample from a mixture of M given Gaussian models, then the probability (pdf) of d given the Gaussian mixture model is given by

$$P(d|\Pi, \Theta) = \sum_{j=1}^{M} \pi_j P(d|\mu_j, C_j), \tag{1}$$

where $\Pi = (\pi_1, \pi_2, \cdots, \pi_M)$ are the mixture proportions and the convex combination requires that $\pi_j \geq 0$ for each $j = 1, 2, \cdots, M$ and $\sum_{j=1}^{M} \pi_j = 1$ [14]. $P(d|\mu_j, C_j)$ is a Gaussian distribution with mean μ_j and covariance matrix C_j. In Eq. 1, $\Theta = (\theta_1, \theta_2, \cdots, \theta_M)$ and $\theta_j = (\mu_j, C_j)$. Let $\Phi = (\Pi, \Theta)$ denote the Gaussian mixture model parameters, then Eq. 1 becomes

$$P(d|\Phi) = \sum_{j=1}^{M} \pi_j P(d|\theta_j). \tag{2}$$

In the current research setting, we assume that seismic data of each geological facies follow a Gaussian probability distribution, therefore, the seismic data of the whole reservoir, which is composed of several facies, are samples of a Gaussian mixture model. To identify geological facies from seismic data, we need to find the Gaussian models and the model from which each datum is sampled.

3 EM algorithm

Suppose a set of measurements $D = (d_1, d_2, \cdots, d_N)$ are samples from a given Gaussian mixture model, Eq. 2. The log-likelihood function of the Gaussian model parameters Φ with data D is

$$L(\Phi|D) = \log P(D|\Phi), \tag{3}$$

where the log denotes natural logarithm. If we know from which Gaussian model each datum is sampled, i.e. the grouping of the data is known, we can easily determine the maximum likelihood estimate of Φ. This is called the complete-data problem. However, we generally have only data, but no information on the grouping. In this case, determining the Gaussian model parameters Φ becomes an incomplete-data problem. This incomplete-data problem can be solved iteratively using an Expectation-Maximization (EM) algorithm.

As is shown in [14] and [23], the log-likelihood function can be written as

$$L(\Phi|D) = Q(\Phi|\Phi_n) + R(\Phi|\Phi_n), \tag{4}$$

where Φ_n are the Gaussian model parameters from the previous (nth) iteration. And Q is the expectation of the complete-data likelihood function given by

$$Q(\Phi|\Phi_n) = E_Z\{\log\left[P(D, Z|\Phi)\right]|D, \Phi_n\}, \tag{5}$$

and R is the difference between the incomplete-data log-likelihood (Eq. 3) and the complete-data log-likelihood (Q-function). $Z = (z_1, z_2, \cdots, z_N)$ where z_i is a group indicator for datum d_i. If datum d_i belongs to the jth group, i.e. it is sampled from the jth Gaussian model, then $z_i = j$.

It is difficult to obtain the maximum likelihood estimate of the Gaussian mixture model parameters Φ by directly maximizing the incomplete-data log-likelihood function of Eq. 3. Instead, the EM algorithm iteratively improves the incomplete-data log-likelihood function by increasing the Q-function (the expectation of the complete-data log-likelihood function) at each iteration. It is shown in [14] that if the Q-function is increased at each iteration, then so will be the incomplete-data log-likelihood function $L(\Phi|D)$. It can be shown in [14] that Eq. 5 is equivalent to

$$Q(\Phi|\Phi_n) = \sum_{i=1}^{N} \sum_{j=1}^{M} h_i^j(\Phi_n) \log\left[\pi_j P(d_i|\delta_i^j = 1, \Phi)\right], \tag{6}$$

where $\delta_i^j = 1$ if $z_i = j$; and is equal to 0 if $z_i \neq j$. $h_i^j(\Phi_n)$ is the expectation of δ_i^j with given data and Gaussian mixture model parameters (Φ_n) at the nth iteration, i.e.,

$$\begin{aligned} h_i^j(\Phi_n) &= E_Z\{\delta_i^j | D, \Phi_n\} \\ &= P(\delta_i^j = 1 | d_i, \Phi_n) \\ &= \frac{(\pi_j)_n P(d_i|(\mu_j)_n, (C_j)_n)}{\sum_{k=1}^M \{(\pi_k)_n P(d_i|(\mu_k)_n, (C_k)_n)\}}, \end{aligned} \tag{7}$$

where

$$P(d_i|(\mu_j)_n, (C_j)_n) = \frac{1}{(2\pi)^{\frac{N_d}{2}} |(C_j)_n|^{\frac{1}{2}}} \cdot \exp\Big[-\frac{1}{2}(d_i - (\mu_j)_n)^T (C_j)_n^{-1} (d_i - (\mu_j)_n)\Big]. \tag{8}$$

In Eq. 8 N_d is the dimension of the data vector d_i and $|(C_j)_n|$ is determinant of the covariance matrix $(C_j)_n$. At the $(n+1)$st iteration, the E-step calculates the membership matrix using Eq. 7 together with Eq. 8. From Eq. 7, we can see that $h_i^j(\Phi_n)$ defines the probability of the ith datum belonging to the jth group (ith datum sampled from the jth Gaussian model), which is the grouping information of the data. The membership matrix $H = H(\Phi_n)$ at the nth iteration is the $N \times M$ matrix which has $h_i^j = h_i^j(\Phi_n)$ as its entry in the ith row and jth column.

The first step in the EM algorithm is to calculate the entries of the membership matrix, h_i^j, for given Φ_n from Eq. 7. As h_i^j is the expectation of δ_i^j, this step is called the expectation step.

At the maximization step (M-step) of the $(n+1)$st iteration, we need to estimate the Gaussian mixture model parameters Φ_{n+1} by maximizing the Q-function defined in Eq. 6 with the calculated membership matrix (Eq. 7) from the E-step, i.e.

$$\Phi_{n+1} = \arg_\Phi \max Q(\Phi|\Phi_n). \tag{9}$$

As shown in [14], the solutions for the maximization step are,

$$\begin{aligned} (\mu_j)_{n+1} &= \frac{\sum_{i=1}^N (h_i^j)_n d_i}{\sum_{i=1}^N (h_i^j)_n}, \\ (C_j)_{n+1} &= \frac{\sum_{i=1}^N (h_i^j)_n (d_i - (\mu_j)_{n+1})(d_i - (\mu_j)_{n+1})^T}{\sum_{i=1}^N (h_i^j)_n}, \\ (\pi_j)_{n+1} &= \frac{1}{N} \sum_{i=1}^N (h_i^j)_n, \end{aligned} \tag{10}$$

where $(h_i^j)_n = h_i^j(\Phi_n)$. These solutions are used to start the next iteration if convergence is not reached.

4 Neighborhood EM (NEM) algorithm

The neighborhood EM (NEM) algorithm improves the spatial continuity of data within each group by adding a spatial penalty term to the original incomplete-data log-likelihood function [2] to obtain U given by

$$U(\Phi|D) = L(\Phi|D) + \beta\, G(H), \tag{11}$$

where β in the penalty term is an adjustable parameter and needs to be determined experimentally. When β is very small, the results of NEM algorithm become similar to those obtained with the standard EM algorithm. When β is too large, then the NEM overemphasizes the spatial continuity of a facies and results in too few facies. The sensitivity study in [11] shows that a value of 0.01 gives reasonable estimates of facies maps for all the examples considered. In the examples of this paper, $\beta = 0.01$ is used. The spatial constraint function $G(H)$ is defined as

$$G(H) = \frac{1}{2} \sum_{k=1}^N \sum_{i=1}^N \sum_{j=1}^M h_i^j h_k^j v_{ik}, \tag{12}$$

where v_{ik} defines the neighborhood, i.e.,

$$v_{ik} = \begin{cases} 1 & \text{if } d_i \text{ and } d_k \text{ are neighbors and } i \neq k, \\ 0 & \text{otherwise.} \end{cases} \tag{13}$$

Here a neighborhood is defined as data points adjacent to each other, e.g. for a 2-D data map, a 3×3 window around the current point is used to define the neighborhood.

NEM is different than the standard EM algorithm in that the entries of the membership matrix include the spatial information of the current data point and its neighbors.

$$\begin{aligned} &(h_i^j)_n \\ &= \frac{(\pi_j)_n P\left(d_i|(\mu_j, C_j)_n\right) \exp(\beta \sum_{k=1}^N h_k^j v_{ik})}{\sum_{j'=1}^M \{(\pi_{j'})_n P(d_i|(\mu_{j'}, C_{j'})_n) \exp(\beta \sum_{k=1}^N h_k^{j'} v_{ik})\}}, \end{aligned} \tag{14}$$

where the spatial term $\exp(\beta \sum_{k=1}^N h_k^j v_{ik})$ acts as a spatial smoothing term on the membership matrix similar to the one in the spatial EM algorithms developed in [25]. Note that h_i^j appears on both sides of Eq. 14, which suggests we should use an iterative algorithm to compute h_i^j. But, we simply use the h_i^j from the previous iteration on the right hand side of Eq. 14 to compute $G(H)$.

Since the spatial term in the augmented log-likelihood function of Eq. 11 does not contain Gaussian mixture model parameters Φ, the maximization with re-

spect to Φ is the same as in the standard EM algorithm. The update on Φ is the same as in Eq. 10.

5 Data grouping during EM iterations

At each EM iteration, we update the group indicator Z by assigning each datum (d_i) to a certain group according to the membership matrix (H). As the entries of the membership matrix represent the probability that each datum is sampled from a certain Gaussian model, we can assign a datum to a group (Gaussian model) that corresponds to the largest probability, i.e. $(z_i) = \ell$ if ℓ is the largest entry in the ith row of the membership matrix, $\{h_i^j,\ j = 1, 2, \cdots, M\}$, which is referred to as the MAP estimate of the group indicator Z. The group indicator Z can also be assigned stochastically by sampling the cumulative distribution function for the ith row of the current membership matrix [25].

In the standard EM and NEM algorithms, the number of groups (M) do not change during the iterations. Therefore, when the EM algorithms are applied for seismic facies classification, we need to know a priori the number of facies in the system and assign this number as the number of groups. However, it is usually difficult to estimate the number of seismic facies in the system a priori. In the EM algorithms applied in this research, we start with a large number of groups and gradually eliminate the small groups during iterations. Two criteria have to be satisfied when a group is eliminated: 1) no data fall into that group according to the group indicator Z; 2) the Gaussian mixture model proportion π_j for that group is less than a prescribed small value (we use 0.0001 for the examples in the paper).

6 Convergence criteria

The EM iteration is terminated when 1) no groups are eliminated; and 2) the relative change in Gaussian mixture model proportions is small, i.e., $\frac{\|(\pi_j)_{n+1}-(\pi_j)_n\|}{\|(\pi_j)_n\|} < \epsilon$ for $j = 1, 2, \cdots, M$. In the examples of this paper we use $\epsilon = 10^{-4}$.

The criteria are tested after each maximization step. If both of them are satisfied, iteration stops. Otherwise, we do the next iteration.

7 Examples

In the following two synthetic examples, we apply the standard EM algorithm, the NEM algorithm and a spatial EM algorithm from [25] to identify facies from seismic attribute measurements. In both examples, we use two types of seismic data: acoustic impedance and Poison's ratio simultaneously.

7.1 Example 1

This example pertains to identifying channel sands from seismic attributes (acoustic impedance and Poison's ratio). The facies map for this synthetic case is shown in Fig. 1 and generated with multipoint geostatistics using the software SNESIM [6]. The red color represents the high porosity channel sand facies with low shaliness and the black color is the low porosity mudstone facies with high shaliness. The grid system is 100 × 100 and the average width of the channel is about 6 grid blocks and the channel facies occupies 30% of the system. Heterogeneous porosity and shaliness distributions are assigned to both the channel and non-channel facies with prescribed variograms. The acoustic impedance and Poison's ratio are calculated using the same rock physics model used in [10]. The generated synthetic seismic attributes are shown in Fig. 2 with measurement errors added. From the measurements of Poison's ratio (Fig. 2a) and acoustic impedance (Fig. 2b), we can vaguely see the structure of the channel sand.

In the EM algorithms, the initial grouping can be generated according to value (amplitude), spatial locations or randomly. All the examples in the paper use random initial grouping. First, we assume that we know the number of facies in the system and fix the initial number of groups to the correct number of facies in the system. Fig. 3a shows the initial random grouping. The red and black colors represent the two initial groups

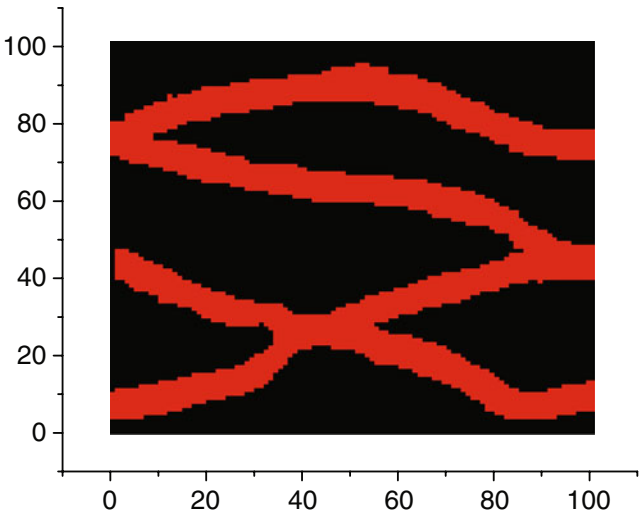

Fig. 1 Facies map, example 1

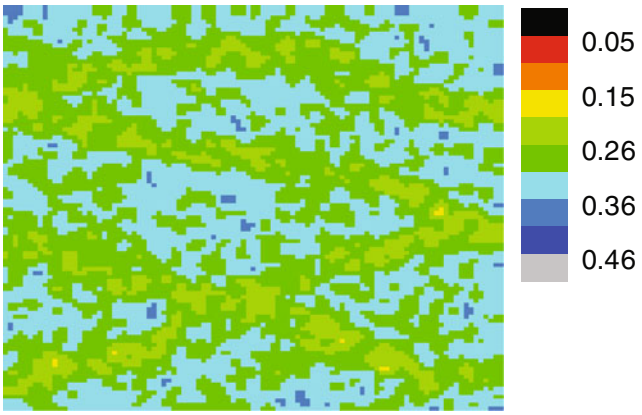

(a) Poison's ratio

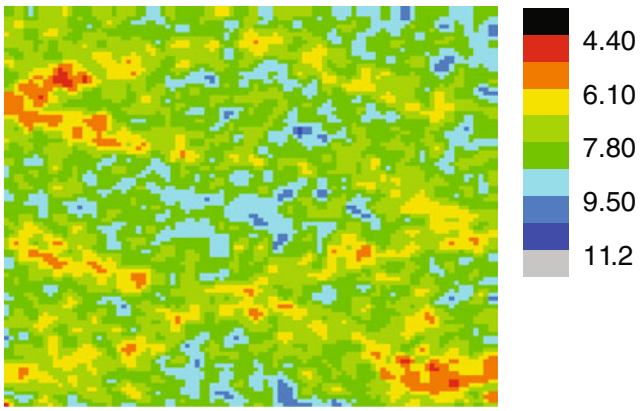

(b) Acoustic impedance

Fig. 2 Seismic attribute measurement, example 1

(facies). Starting with this random grouping, we have obtained the final groups using the three EM algorithms (Fig. 3b for the standard EM algorithm, Fig. 3c for the NEM algorithm and Fig. 3d for the spatial EM algorithm). It can be seen that all the EM algorithms can obtain the final grouping corresponding to the true facies map (Fig. 1) using the seismic data. The final grouping from different EM algorithms are quite similar and the EM algorithms with spatial constraints (NEM and the spatial EM) do not show any significant advantages over the standard EM algorithm in this case although the spatial EM yields slightly more continuous facies.

Figure 4 shows the initial random grouping together with the final grouping of the three different EM algorithms when we start with 10 random initial groups. Although we have modified the standard EM algorithm to allow small groups to be eliminated, only one group was eliminated and the final number of groups is 9. The major structure of the channel sand is shown in red and is well identified. However, the mudstone facies is

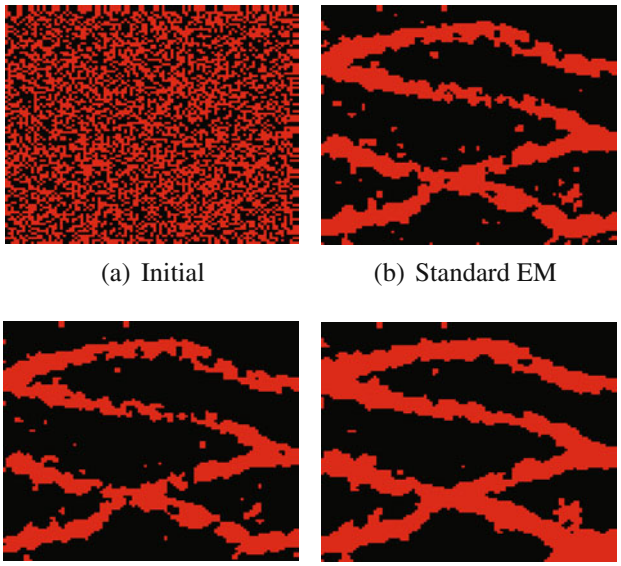

(a) Initial (b) Standard EM

(c) NEM (d) Spatial EM

Fig. 3 Initial and final facies maps with 2 random initial groups, example 1

divided into 8 small isolated groups due to the fact that this EM algorithm does not consider the spatial relationship among data points. The NEM and spatial EM algorithms eliminated more small groups and obtained better final grouping and hence better facies maps.

In the truth case, the proportion of the channel facies (red color in Fig. 1) is 30%, while the proportion of the non-channel facies is 70%. Here, the proportion is defined as the percentage of the pixels of each facies

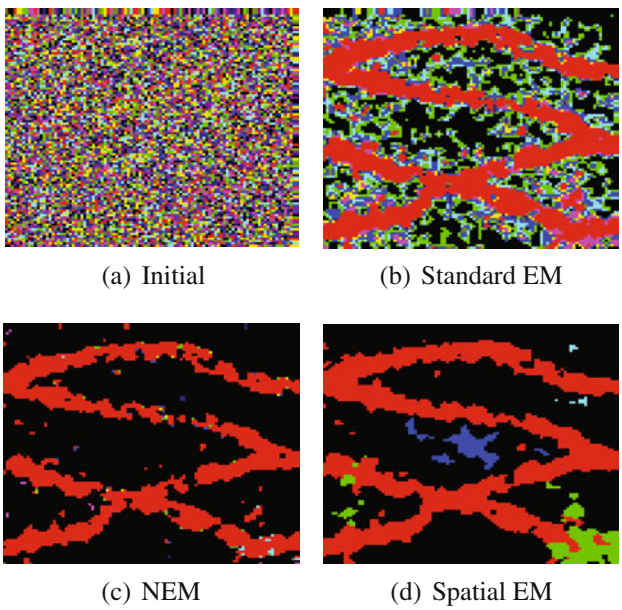

(a) Initial (b) Standard EM

(c) NEM (d) Spatial EM

Fig. 4 Initial and final facies maps with 10 random initial groups, example 1

Table 1 Estimated facies proportions (FP) in example 1

Example 1		TRUE	EM	NEM	Spatial EM
Initial 2 groups	Channel FP	30%	30%	27%	34%
	Non-Channel FP	70%	70%	73%	66%
Initial 10 groups	Channel FP	30%	30%	25%	30%
	Non-Channel FP	70%	26%	74%	64%

in the facies map. Table 1 shows the estimated facies proportions by the three different EM algorithms compared to the truth. When we start with 2 initial groups, all the EM algorithms yield reasonable estimate of the facies proportions (FP). Note that the standard EM algorithm coincidentally yields the exact facies proportions: 30% for the channel facies and 70% for the non-channel facies as the truth case. When the initial number of groups is 10, the NEM and spatial EM algorithms obtained reasonable facies proportion for both the channel and non-channel facies. The standard EM algorithm could only estimate the channel facies proportion reasonably well and the non-channel facies is divided into 9 small groups and the largest one among the 9 groups only has a proportion of 26%. Table 2 shows the facies identification success rate (FISR). The total FISR is the percentage of the pixels whose facies are correctly identified. The channel FISR is the percentage of the pixels among the channel facies that are correctly identified as channel facies. When the number of initial groups is 2, which is the right number of facies, the total FISR is above 90% for the three EM algorithms. However, the spatial EM yields a better channel FISR of 93% and NEM has the worse channel FISR of 79%. This is also shown in the estimated facies map of Fig. 3, in which the estimated channel facies from the standard EM and NEM is not as continuous as that of the spatial EM algorithm. When we start with 10 initial groups, EM has a much smaller total FISR as the non-channel facies is divided into 9 small groups, while NEM and spatial EM algorithm have reasonable FISR value.

7.2 Example 2

In Example 2, we added a crevasse facies to the facies map in Example 1. As shown in Fig. 5, the crevasse facies (green color) is 1 or 2 grid blocks wide along the edge of the channel sand. The values of porosity and shaliness of the crevasse facies are between those of the

Table 2 The facies identification successful rate (FISR) in example 1

Example 1		EM	NEM	Spatial EM
Initial 2 groups	Total SR	91%	91%	92%
	Channel SR	85%	79%	93%
Initial 10 groups	Total SR	51%	90%	88%
	Channel SR	85%	76%	86%

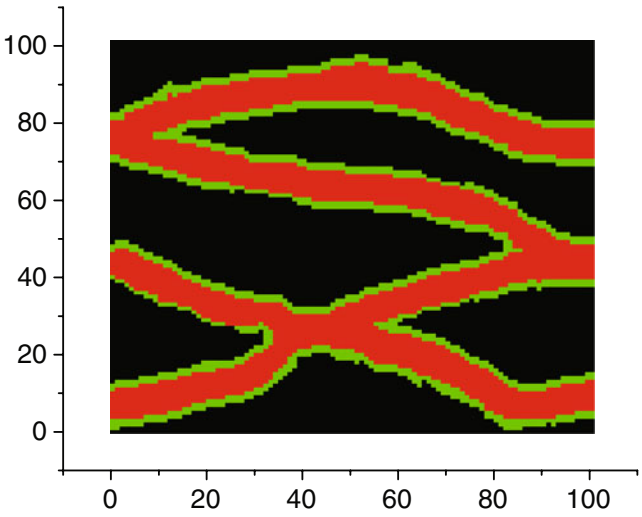

Fig. 5 Facies map, example 2

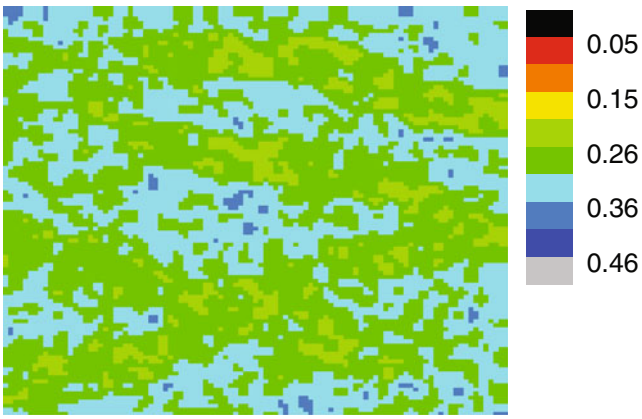

(a) Poison's ratio

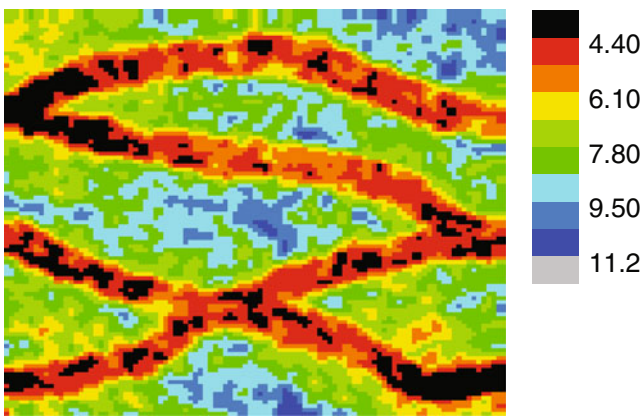

(b) Acoustic impedance

Fig. 6 Seismic attribute measurement, example 2

channel sand (red color) and mudstone (black color) facies. In this example, acoustic impedance shows clearly the channel facies (black and red colors in Fig. 6b) and the Poison's ratio (Fig. 6a) is of similar quality to that in Example 1. The crevasse facies shows up as the yellow color in the acoustic impedance plot (Fig. 6b) while it is obscure in the Poisson's ratio plot (Fig. 6a). In this example, we will test the applicability of the EM algorithms for picking up a long but narrow crevasse facies.

Figure 7 shows the initial random grouping and the final groupings from three different EM algorithms when we start with 3 random initial groups which are shown in red, green and black colors in Fig. 7a. All three EM algorithms clearly identified the channel sand facies shown in red color due to the fairly clear picture of the channel sand in the acoustic impedance measurement. Although the crevasse facies consists only a small proportion of the whole system, the three EM algorithms identify the existence of this facies. However, the standard EM algorithm and the spatial EM algorithm overestimated the proportions of the crevasse facies and the NEM algorithm gives a narrower and discontinuous crevasse facies. When we start with 10 random initial groups (Fig. 8a), all three EM algorithms have limited success in identifying the crevasse facies (Fig. 8b, c and d).

Table 3 shows the estimated facies proportions (FP) by the three different EM algorithms compared to the truth. When we start with 3 initial groups, all the

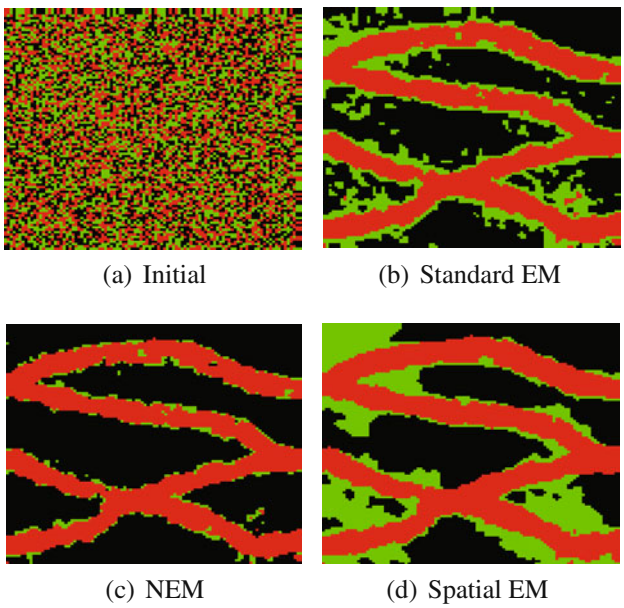

(a) Initial (b) Standard EM

(c) NEM (d) Spatial EM

Fig. 7 Initial and final facies maps with 3 random initial groups, example 2

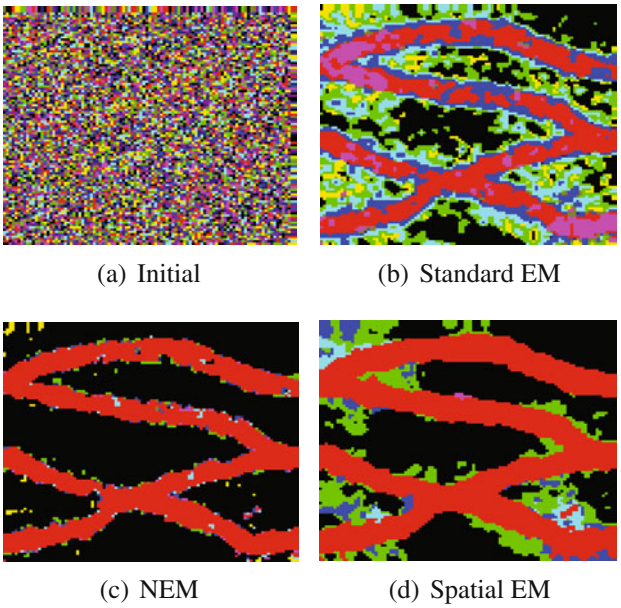

(a) Initial (b) Standard EM

(c) NEM (d) Spatial EM

Fig. 8 Initial and final facies maps with 10 random initial groups, example 2

EM algorithms yield reasonable estimate of the facies proportions (FP) for the channel facies. NEM gives the best estimate of the non-channel facies proportion and lowest estimate of the crevasse facies proportion as can be seen from the estimated facies map in Fig. 7. The spatial EM over-estimated the channel and crevasse facies proportion and under-estimated the non-channel facies proportion. When the initial number of groups is 10, the NEM gives the best estimate on the channel and non-channel facies proportion although it significantly under-estimates the crevasse facies proportion. As shown in Table 4, all three EM algorithms have successfully identified the channel facies with a FISR of above 96%, while the facies identification success rate is quite low for the crevasse facies (EM-66%; NEM-27%; spatial EM-49%) even with 3 initial groups. When we start with 10 initial groups, NEM and spatial EM algorithm could still have high facies identification successful rate but the standard EM has a much smaller value of FISR. However, NEM and spatial EM cannot identify the small crevasse facies, which yields a FISR value around 10%.

Table 3 Estimated facies proportions (FP) in example 2

Example 2		TRUE	EM	NEM	Spatial EM
Initial	Channel FP	30%	34%	33%	37%
3 groups	Non-Channel FP	56%	45%	62%	38%
	Crevasse FP	14%	21%	5%	25%
Initial	Channel FP	30%	22%	32%	40%
10 groups	Non-Channel FP	56%	21%	63%	41%
	Crevasse FP	14%	15%	1%	13%

Table 4 The facies identification successful rate (FISR) in example 2

Example 2		EM	NEM	Spatial EM
Initial	Total SR	83%	88%	74%
3 groups	Channel SR	97%	96%	99%
	Crevasse SR	66%	27%	49%
Initial	Total SR	51%	85%	70%
10 groups	Channel SR	69%	95%	100%
	Crevasse SR	61%	8%	11%

8 Conclusions

In this paper, we applied three different EM algorithms (standard EM, NEM and spatial EM) to identify rock facies from seismic data. The following conclusions are warranted:

1. When the number of geological facies in the system is known and we set the number of initial groups equal to this number, all three EM algorithms give reasonable estimates on the distribution of the facies.
2. When the number of geological facies is not known a priori, we recommend starting with a fairly large number of initial groups. In this case, the standard EM algorithm tends to keep the same number of groups as the initial number and yields incorrect final groups. The spatial EM and NEM algorithms can delete most of the redundant groups and obtain an improved approximation of the distribution of geological facies in the system.
3. The EM algorithms can identify the existence of the crevasse facies visually when the initial number of groups is equal to the number of facies. However, the facies identification success rate is quite low. When the initial number of groups is much larger than the number of facies in the reservoir, the EM algorithms fail to identify the crevasse facies.

Acknowledgements The support of the member companies of TUPREP is very gratefully acknowledged.

References

1. Allard, D., Guillot, G.: Clustering Geostatistical Data, Geostatistics 2000, vol. 1, pp. 49–63. Cape Town (1999)
2. Ambroise, C., Dang, M., Govaert, G.: Convergence of an EM-type algorithm for spatial clustering. Pattern Recogn. Lett. **19**, 919–927 (1998)
3. Aminzadeh, I.F., Chattcsjee, S.: Applications of clustering in exploration seismology. Geoexploration **23**(1), 147–159 (1984)
4. Arpat, B.G., Caers, J., Haas, A.: Characterization of west-Africa submarine channel reservoirs: a neural network based approach to integration of seismic data. In: 2001 SPE Annual Technical Conference and Exhibition (2001)
5. Besag, J.E.: On the statistical analysis of dirty pictures. J. R. Stat. Soc., Ser. B **48**(3), 295–302 (1986)
6. Caers, J.: Petroleum Geostatistics. Society of Petroleum Engineers, Richardson, Texas (2005)
7. Celeux, G., Govaert, G.: A classification EM Algorithm for Clustering and Two Stochastic Versions. Rapports de Recherche (1991)
8. Dempster, A.P., Laird, N.M., Rubin, D.B.: Maximum likelihood from incomplete data via the EM algorithm. J. Roy. Statist. Soc. B **39**(1), 1–38 (1977)
9. Diplaros, A., Gevers, T., Vlassis, N.: Skin detection using the EM algorithm with spatial constraints, systems, man and cybernetics. In: 2004 IEEE International Conference, vol. 4 (2004)
10. Dong, Y., Oliver, D.S.: Quantitative use of 4D seismic data for reservoir description. SPE J. **10**(1), 51–65 (2005)
11. Han, M.: Application of the EM algorithms for facies classfication and measurement error estimation. M.S. Thesis, University of Tulsa, Tulsa, Oklahoma, USA (2008)
12. Hartley, H.: Maximum likelihood from incomplete data. Biometrics **14**(1), 174–194 (1958)
13. John, A., Lake, L.W., Torres-Verdin, C., Srinivasan, S.: Seismic facies identication and classication using simple statistics. SPE Reserv. Evalu. Eng. **11**(6), 984–990 (2005)
14. Kung, S., Mak, M., Lin, S.: Biometric Authentication: A Machine Learning Approach. Prentice Hall (2004)
15. Liu, N., Oliver, D.S.: Critical evaluation of the ensemble Kalman filter on history matching geological facies. SPE Reserv. Evalu. Eng. **8**(4) 470–477 (2005)
16. Meng, X.-L.: On the rate of convergence of the ECM algorithm. Ann. Stat. **22**(1), 326–339 (1994)
17. Ng, I., Kittler, J., Illingworth, J.: Supervised segmentation using a multiresolution data representation. Signal Process. **3**, 36–44 (1993)
18. Pitas, I., Kotropoulos, C.: A texture-based approach to the segmentation of seismic images. Pattern Recogn. **25**, 929–945 (1992)
19. Redner, R.A., Walker, H.F.: Mixture densities, maximum likelihood and the EM algorithm. SIAM Rev. **26**(2), 195–239 (1984)
20. Tang, H., Ji, H.: Incorporation of spatial characteristics into volcanic facies and favorable reservoir prediction. In: 2004 SPE Annual Technical Conference and Exhibition (2004)
21. Teixeira, R., Braga, I., Loures, L.: Bayesian characterization of subsurface lithofacies and saturation fluid. In: 2007 SPE Latin American and Caribbean Petroleum Engineering Conference (2007)
22. Wiseman, S.: Seismic image segmentation. In: 1999 European Assoc. of Geoscientists and Engineers Conference (1999)
23. Zhao, Y., Li, G., Reynolds, A.C.: Characterizing the measurement error with the EM algorithm. In: Proceedings of 10th European Conference on the Mathematics of Oil Recovery (2006)
24. Zhao, Y., Li, G., Reynolds, A.C.: Generating facies maps by assimilating production data and seismic data with the ensemble Kalman filter. In: Proceedings of 2008 SPE/DOE Improved Oil Recovery Symposium (2008)
25. Zhao, Y., Li, G., Reynolds, A.C.: Characterization of the measurement error in time-lapse seismic data and production data with an EM algorithm. Oil Gas Sci. Technol. - Rev. IFP **62**(2), 181–193 (2007)